JOURNAL OF Applied Polymer SCIENCE

Poly(ε-caprolactone) Composite Scaffolds Loaded with Gentamicin-Containing β-Tricalcium Phosphate/Gelatin Microspheres for Bone Tissue Engineering Applications

Umran Aydemir Sezer,[1,2,3] Damla Arslantunali,[1,4,5] Eda Ayse Aksoy,[1,6] Vasif Hasirci,[1,2,5,7] Nesrin Hasirci[1,2,5,8]

[1]BIOMATEN, Center of Excellence in Biomaterials and Tissue Engineering, Middle East Technical University, Ankara 06800, Turkey
[2]Graduate Department of Biomedical Engineering, Faculty of Arts and Sciences, Middle East Technical University, Ankara 06800, Turkey
[3]Department of Chemical Engineering and Applied Chemistry, Faculty of Engineering, Atilim University, Ankara 06836, Turkey
[4]Department of Bioengineering, Faculty of Engineering, Gümüşhane University, Gümüşhane 29100, Turkey
[5]Department of Biotechnology, Faculty of Arts and Sciences, Middle East Technical University, Ankara 06800, Turkey
[6]Department of Basic Pharmaceutical Sciences, Faculty of Pharmacy, Hacettepe University, Ankara 06100, Turkey
[7]Department of Biological Sciences, Faculty of Arts and Sciences, Middle East Technical University, Ankara 06800, Turkey
[8]Department of Chemistry, Faculty of Arts and Sciences, Middle East Technical University, Ankara 06800, Turkey
Correspondence to: N. Hasirci (E-mail: nhasirci@metu.edu.tr)

ABSTRACT: In this study, novel poly(ε-caprolactone) (PCL) composite scaffolds were prepared for bone tissue engineering applications, where gentamicin-loaded β-tricalcium phosphate (β-TCP)/gelatin microspheres were added to PCL. The effects of the amount of β-TCP/gelatin microspheres added to the PCL scaffold on various properties, such as the gentamicin release rate, biodegradability, morphology, mechanical strength, and pore size distribution, were investigated. A higher amount of filler caused a reduction in the mechanical properties and an increase in the pore size and led to a faster release of gentamicin. Human osteosarcoma cells (Saos-2) were seeded on the prepared composite scaffolds, and the viability of cells having alkaline phosphatase (ALP) activity was observed for all of the scaffolds after 3 weeks of incubation. Cell proliferation and differentiation enhanced the mechanical strength of the scaffolds. Promising results were obtained for the development of bone cells on the prepared biocompatible, biodegradable, and antimicrobial composite scaffolds. © 2013 Wiley Periodicals, Inc. J. Appl. Polym. Sci. **2014**, *131*, 40110.

KEYWORDS: biodegradable; biomaterials; composites; foams

Received 23 July 2013; accepted 23 October 2013
DOI: 10.1002/app.40110

INTRODUCTION

Bone tissue engineering has become an expanding research area as a new and promising approach for bone repair and regeneration. Constructions of scaffolds that mimic the properties of the target tissue are major challenges to tissue engineering.[1] The requirements for ideal scaffold construction are sufficient porosity, pore dimensions, and pore interconnectivity for initial cell attachment and tissue ingrowth with nutrient and cell waste transportation,[2] biocompatibility, biodegradability, and mechanical strength; the scaffolds need to show a similar degradation rate and mechanical properties as the targeted tissue.[3] Scaffold design for bone tissue engineering can be assigned as more challenging because the scaffold should be strong enough to offer adequate support for bone tissue in addition to a sufficient porosity to guide bone ingrowth.[2] As bone tissue has a composite structure containing elastic collagen and stiff hydroxyapatite, studies have focused on composite scaffolds mainly containing a biodegradable elastic polymer and stiff additives, which can be various bioceramics fillers to increase the mechanical strength.[4]

Poly(ε-caprolactone) (PCL) is a polymer used in medical applications either as hard-tissue supports or as scaffolds for bone tissue engineering. PCL is a hydrophobic polymer, and its surface is not active enough for the cells to attach and proliferate.[5–7] Therefore, modifications with other materials such as bioceramics and polymers can be applied to improve its biocompatibility, hydrophilicity, and degradation rate.[8,9] *In vivo*

Table I. Composition of the PCL Scaffolds

Sample	Type and amount of filler in the PCL scaffolds
PCL-0	Pure PCL with no filler
PCL-10β/G	10 wt % gentamicin-loaded β-TCP–gelatin microsphere
PCL-30β/G	30 wt % gentamicin-loaded β-TCP–gelatin microsphere
PCL-50 β/G	50 wt % gentamicin-loaded β-TCP–gelatin microsphere
PCL-30β/G-ng	30 wt % β-TCP–gelatin microsphere with no gentamicin (ng)
PCL-50β/G-ng	50 wt % β-TCP–gelatin microsphere with no gentamicin (ng)

studies of PCL-based bone scaffolds have indicated bone formation and remodeling in biological media.[10–12]

Beta-Tricalcium phosphate (β-TCP) is a hydrophilic bioceramic, which has osteoconductive and slow resorption properties.[13] Its combination with a PCL scaffold would improve the mechanical and osteoconductive properties, but direct addition into the matrix may result in the fast spreading of the powder because of the poor interaction between TCP and the polymer matrix.[14] The incorporation of β-TCP with a biocompatible polymer can be suggested to have more stable composite structures. Gelatin is a highly hydrophilic biocompatible and biodegradable natural polymer, and it is used widely in biomedical applications, such as drug-delivery systems and scaffolds.[15,16] Therefore, the preparation of microparticles containing both gelatin and β-TCP can prevent the fast spreading of inorganic powder and can improve the biocompatibility of the particles. The incorporation of β-TCP/gelatin particles as fillers into PCL can produce highly bioactive scaffolds because TCP has osteoconductive properties and gelatin has a natural protein structure. Loading a drug into the microparticles can also lead to controllable release with pharmaceutical activity.

One of the major problems associated with the use of implants or scaffolds for bone treatment is the occurrence of infections.[17] To prevent bone infection after an implantation operation, generally an antibiotic such as gentamicin, which has a broad spectrum of activity against both Gram-positive and Gram-negative bacteria, is used.[18] In the literature, there are articles explaining the addition of antibiotics either in the scaffolds during preparation[19] or on the scaffold by adsorption.[20] However, the addition of bioactive agents in microspheres or nanospheres and then the combination with the scaffold material is a more novel technique. Meanwhile, the presence of these particles can improve the performance and orthopedic repair actions of the scaffold.[21–23]

In this study, novel composite scaffolds composed of PCL and gentamicin-loaded β-TCP/gelatin microspheres were prepared for bone tissue engineering. These multifunctional scaffolds demonstrated osteoconductivity initiated by β-TCP, antibacterial activity supplied by gentamicin and biocompatibility and biodegradability resulting from gelatin and PCL. The morphological characteristics, mechanical properties, pore size distribution, degradation, and gentamicin release characteristics were investigated. These novel scaffolds were also tested *in vitro* by the seeding of human osteosarcoma cells (Saos-2), and the cell adhesion, proliferation, and alkaline phosphatase (ALP) activities were studied.

EXPERIMENTAL

Materials

Gelatin was purchased from Sharlau (Spain). Vegetable oil was obtained from Kristal Corn Oil (Turkey). Glutaraldehyde (50% w/w) was purchased from BDH, Ltd. (Poole, United Kingdom). Gentamicin (80 mg/mL) was obtained I. E. Ulagay (Turkey). Phosphate buffer solution (PBS; pH 7.4, 0.1*M*) was prepared with K_2HPO_4 and KH_2PO_4 of Merck Chemicals, Ltd. (Germany). PCL was obtained from Sigma-Aldrich (weight-average molecular weight = 80,000). 1,4-Dioxane was purchased from Carlo Erba (Italy). Thiazolyl blue tetrazolium bromides, bovine serum albumin, sodium cocodylate, and glutaraldehyde (25%) were purchased from Sigma-Aldrich. RPMI-1640 cell culture medium with 2.05 m*M* L-glutamine and phenol red, fetal bovine serum (FBS), penicillin/streptomycin, and trypsin solution (0.25% w/v in Hanks' Balanced Salt Solution, including ethylene diamine tetraacetic acid) were purchased from Hyclone. Dimethyl sulfoxide and Triton X 100 were obtained from AppliChem (Germany). Trypan blue (0.4%) was purchased from Invitrogen, Inc. Saos-2 cell lines were from ATCC. A SensoLyte p-Nitrophenyl phosphate (pNPP) assay kit was purchased from Anaspec.

Methods

Preparation of Gentamicin-Loaded β-TCP/Gelatin Microspheres. Gentamicin-loaded β-TCP/gelatin microspheres were prepared with a water-in-oil emulsion method as previously reported.[24] Shortly, β-TCP powder was added to the gelatin solution under continuous stirring. The ratio of β-TCP/gelatin was 0.5/1 w/w. This suspension was added dropwise into 60 mL of oil (ca. 2200 rpm) and stirred for 30 min. An aqueous Glutaraldehyde (GA) solution (2%, 2 mL) was added dropwise to the medium as a crosslinking agent, and stirring was continued for 20 min. The mixture was cooled to 4°C, washed with acetone, and dried at room temperature. To load gentamicin into microspheres, a gentamicin solution (0.5 mL containing 40 mg of gentamicin) was added to the β-TCP/gelatin microspheres (100 mg) through the application of a vacuum-pressure cycle.

Preparation of Composite Scaffolds Containing Gentamicin-Loaded β-TCP/Gelatin Microspheres. Gentamicin-loaded β-TCP/gelatin microspheres (10, 30, or 50 wt %) were added to the PCL solution (5% prepared in 1,4-dioxane) and stirred for 6 h to obtain a homogeneous dispersion. The mixtures were poured into two different cylindrical molds (with dimensions of diameter (d) = 10 mm and height (h) = 10 mm and d = 5 mm and h = 5 mm, respectively) frozen at −20°C and lyophilized at −80°C. Pure PCL scaffolds and composite scaffolds without gentamicin were also prepared as control groups with the same procedure. Table I summarizes the composition of the scaffolds.

Material Characterization. The morphology of the scaffolds was characterized by scanning electron microscopy (SEM). The scanning range of the samples was 20–40° and the scanning

speed was 2°/min. SEM analyses were performed with a JSM-6400 electron microscope (JEOL). The samples were sputter-coated by an Au thin film before the SEM investigations.

Compressive tests were carried out on a mechanical testing machine (Lloyd Instruments, Ltd., Fareham, United Kingdom), equipped with a 100-N load cell, with a crosshead speed of 10 mm/min. Samples were prepared in molds 10 mm in diameter and 10 mm in height. The load deformation curve was printed for each specimen. Young's modulus was calculated by the multiplication of the load applied per unit area and the deformation per unit length as the slope of the initial linear portion of the stress–strain curve. The compressive strengths (CSs) for the deformation of 50% of the scaffolds (in height) were calculated from the stress–strain curve at which point the stress (CS) met 5 mm of deformation. For each type of sample, at least eight experiments were carried out to determine the reproducibility. The compression tests were conducted for both the dry and wet states. For the wet-state analysis, the scaffolds were immersed in PBS for 24 h before the tests, whereas the lyophilized scaffolds were used for the dry state.

The average pore sizes of the scaffolds were measured with SEM images. The width of each pore was measured with a caliper in the SEM images, and the average values were calculated for each sample. The pore size distribution curves of the composite scaffolds were examined with mercury intrusion porosimetry (Quantachrome). The calculations were replicated for five scaffolds, and the results are expressed as the means plus or minus the standard deviations. Tests were performed under low-pressure conditions in the range 0–50 psi. The contact angle of mercury on PCL was 140°, and the mercury surface tension was 480 ergs/cm^2.

***In Vitro* Gentamicin Release from the Composite Scaffolds.** *In vitro* gentamicin release from the composite scaffolds ($d = 5$ mm and $h = 5$ mm) was carried out in PBS at 37°C. Each sample was placed in a vial and was placed in 5 mL of PBS solution. To prevent UV absorption of the degradation products at the same wavelength with gentamicin, PCL scaffolds containing β-TCP/gelatin microspheres with no gentamicin (PCL-β/G-ng) were also incubated as blanks. The vials were placed in a shaker bath at 100 rpm at 37°C. The medium was taken out at predetermined time intervals, and fresh PBS solution (5 mL) was added. The released amount of gentamicin was detected by an ultraviolet–visible spectrometer from the absorbance at 256 nm and with a calibration curve prepared with known concentrations of gentamicin solutions. The experiments were tripled.

***In Vitro* Degradation Studies.** The hydrolytic and enzymatic degradation studies were carried out for the selected PCL-30β/G samples. Composite scaffolds were prepared as cylinders (5 mm in height and 5 mm in diameter). The hydrolytic degradation studies of the matrices were carried out at 37°C in PBS. For the enzymatic degradation studies, 0.5 mg of lipase was added to 5 mL of PBS and used as the enzymatic degradation medium. The solutions of each sample were replaced with fresh ones every 24 h. For each case, the solutions were drawn out, and the samples were washed with distilled water, freeze-dried, and weighed. We compared the loss in weight gravimetrically by comparing the dried and initial weights of the samples. The morphological changes of the hydrolytically and enzymatically degraded samples (after 1 week) were also investigated by SEM. The physical changes and alterations in porosity were studied.

Human Osteosarcoma (Saos-2) Cell Culture. The Saos-2 cells were cultured in a growth medium that contained RPMI-1640 cell culture medium, FBS (10% v/v), and penicillin/streptomycin (100 units/mL:100 μg/mL, respectively) at 37°C in a CO_2 incubator (Sanyo Incusafe MCO-17AC, Sanyoelectric Co, Japan). Every 2 days, the growth medium was replaced. For trypsin treatment, the attached cells were washed with PBS after the medium was discarded and then incubated with trypsin–ethylene diamine tetraacetic acid (diluted to 0.05% from a 0.25% stock in PBS) at 37°C for 5 min. The detached cells were collected with RPMI-1640 cell culture medium containing 10% serum and penicillin/streptomycin (100 units/mL/100 μg/mL).

Seeding of the Saos-2 Cells on the Composite Scaffolds. The composite scaffolds (PCL-0, PCL-30β/G, PCL-50β/G, PCL-30β/G-ng, and PCL-50β/G-ng) were transferred into sterile 24-well tissue culture polystyrene (TCPS) plates. They were sterilized by the exposure of both sides to UV in a laminar flow hood for 45 min at room temperature. Saos-2 cells were detached from the TCPS flasks, and 20,000 cells were seeded onto each composite scaffold and on the TCPS surface (as control) and incubated for 20 min at 37°C in a CO_2 incubator, and then, 1.5 mL of RPMI-1640 growth medium with FBS (10% v/v) and penicillin/streptomycin (with final concentrations of 100 units/mL and 100 μg/mL, respectively) were added to each well. The medium was replaced every 2 days.

Determination of the Cellular Viability on the Composite Scaffolds by an MTT Assay. The viability and proliferation of the cells were determined by an 3-(4, 5-dimethylthiazolyl-2)-2,5-diphenyltetrazolium bromide (MTT) cell viability assay conducted on days 1, 7, 14, and 21 of cell culturing. At each time point, the scaffolds were moved to another 21-well plate and washed with PBS. Then, the MTT solution prepared by the dissolution of thiazolyl blue tetrazolium bromide in PBS (1 mg/mL) was added and incubated for 3 h at 37°C in a CO_2 incubator. The formed formazan crystals were dissolved with 4% HCl containing isopropyl alcohol. After 1 h of incubation at room temperature with regular shaking, the absorbances at 550 nm were measured with an ultraviolet–visible spectrophotometer (Thermo Scientific, Multiscan Spectrum). A calibration curve was used to calculate the cell numbers using three different samples ($n = 3$).

Determination of the Alkaline Phosphatase Activity of Saos-2 Cells on the Composite Scaffolds. The ALP activity of Saos-2 cells on the composite scaffolds was measured at the end of days 1 and 21 of the incubation period. The assay was conducted according to the manufacturer's instructions with some modifications. The cell extracts from the composite scaffolds were prepared as follows: the cells were washed with an assay buffer (prepared from the manufacturer's protocol by the dilution of a 10× assay buffer to 1× with deionized water). The scaffolds were transferred to sterile 15-mL falcon tubes. The lysis buffer supplied with the ALP assay kit (Triton X-100 in assay buffer, 2:1000 v/v) were added. The scaffolds were frozen at −20°C, thawed at 37°C three times, and then sonicated on

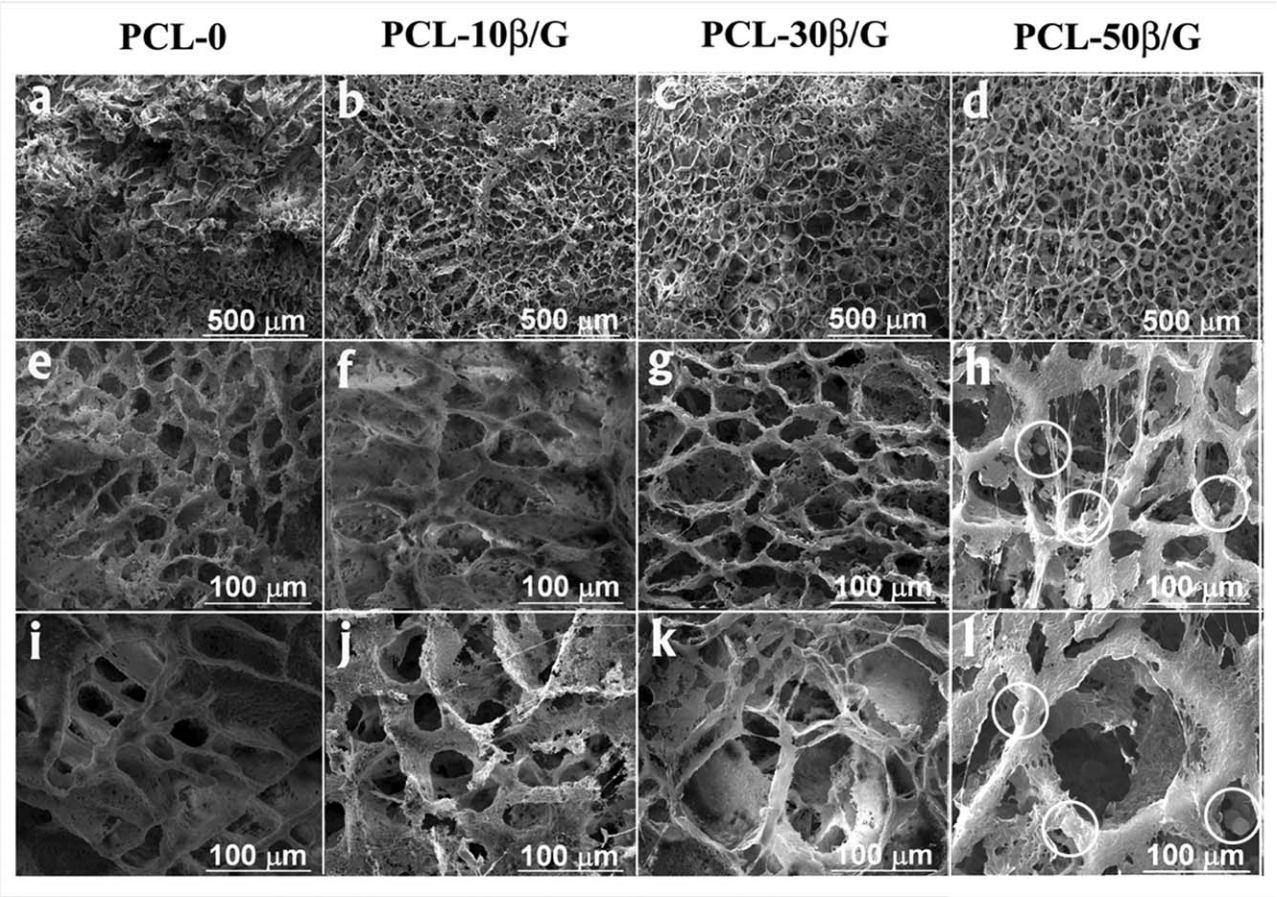

Figure 1. SEM images of the scaffolds: surfaces of (a) PCL-0, (b) PCL-10*β*/G, (c) PCL-30*β*/G, (d) PCL-50*β*/G with low magnification, (e) PCL-0, (f) PCL-10*β*/G, (g) PCL-30*β*/G, and (h) PCL-50*β*/G with high magnification and cross sections of (i) PCL-0, (j) PCL-10*β*/G, (k) PCL-30*β*/G, and (l) PCL-50*β*/G with high magnification.

ice until the scaffolds ruptured. They were centrifuged at 2000 rpm for 10 min. Fifty microliters of the supernatant were transferred to a 96-well TCPSs and diluted (1:1) with a dilution buffer. Fifty microliters of *p*-nitrophenylphosphate (supplied with the kit) was added and incubated for 60 min at 37°C. Fifty microliters of stop solution was added, and the absorbances were measured at 405 nm. The ALP activity was calculated with a calibration curve.

SEM. The behavior of the cells on scaffolds was studied by SEM. The scaffolds were removed from media and washed twice with PBS. Then, cocodylate buffer (0.1*M* sodium cacodylate, pH 7.4) was used for the last washing and incubated in glutaraldehyde (2.5% v/v in cocodylate buffer, Sigma-Aldrich) at room temperature for 2 h. After they were washed with cocodylate buffer, the samples were freeze-dried for 2–3 h and coated with Au *in vacuo* and examined with SEM (JEOL, JSM-6400) at 5–10 kV.

Effect of the Saos-2 Cells on the Mechanical Properties of the Composite Scaffolds. The cells were seeded on PCL-30*β*/G and PCL-50*β*/G composite scaffolds as described before. After 21 days of incubation, the cells were fixed with 4% v/v paraformaldehyde for 15 min at room temperature; this was followed by washing with PBS. Similar scaffolds were also incubated in the feeding medium without the addition of cells as control groups. After 21 days of incubation, the scaffolds were tested in the wet state, and the ones with cells were also tested after drying. Compressive tests were carried out as described in the Material Characterization section.

Statistical Analysis. All of the characterization and *in vitro* studies were performed in triplicate. A one-tail student's *t* test, with standard Microsoft Excel software, was used to determine the significant differences between the mean values in the control and test groups. The differences obtained were considered statistically significant for *p* values equal to or smaller than 0.05.

RESULTS AND DISCUSSION

Characterization of the Composite Scaffolds

The microstructure of the pure PCL (PCL-0) and composite PCL scaffolds are indicated in Figure 1. PCL-0 appeared to have a bulk and closed pore structure on the surface, whereas open pores were observed in the inner part of the scaffolds [Figure 1(a,e,i)]. In the PCL-10*β*/G samples, bulk and closed regions were observed [Figure 1(b,f,j)] with open microporous structures. With increasing amount of fillers, these bulk regions disappeared. Moreover, with increasing filler ratio in the three-

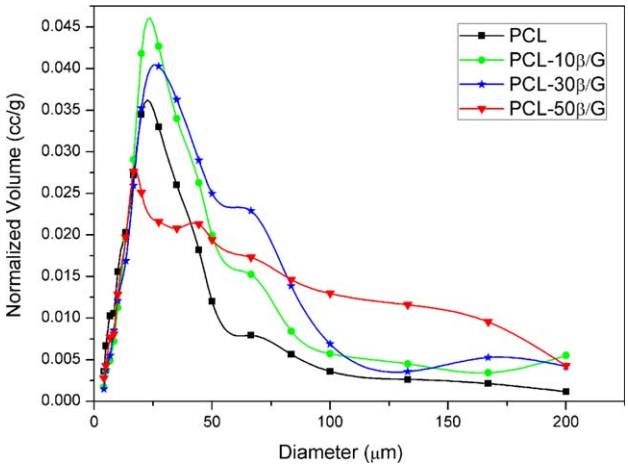

Figure 2. Pore size distributions of the PCL scaffolds. [Color figure can be viewed in the online issue, which is available at wileyonlinelibrary.com.]

dimensional matrices, interconnected open and larger pore structures were obtained, and the pore dimensions and interconnectivity increased both on the surface and inner surface of the composite scaffolds. All of the samples showed smaller pores on the surface and larger pores in the bulk of the matrices.

The pore structure of the PCL composite scaffolds incorporated with the composite microspheres appeared different than that of pure PCL scaffolds. The composite scaffolds demonstrated thinner honey comblike structures, and fibers within the pores were observed in the presence of the fillers [Figure 1(j,g,h)]. Similar morphological characteristics were observed for the two-dimensional matrices composed of PCL and β-TCP/gelatin microspheres after enzymatic degradation.[25] The microspheres were embedded in the PCL matrices homogeneously; however, free microspheres could be seen within the pores [Figure 1(h,l)]. According to the SEM images, the average pore sizes were 33, 40, 100, and 160 μm for PCL, PCL-10β/G, PCL-30β/G, and PCL-50β/G, respectively. This phenomenon could be attributed to the increasing inhomogeneity with microsphere addition and increased incompatibility between the hydrophilic filler and the hydrophobic PCL matrix.[26] As a result, the microspheres can be used as fillers to obtain porous scaffolds with PCL without any porogen, and PCL-30β/G and PCL-50β/G may be good candidates for bone tissue engineering applications.

Porosity and pore size distribution are important factors in the success of tissue engineering applications. Many studies have focused on the detection of optimal values for these factors. However, there are still contradictory results for the pore size distributions required for cell attachment and proliferation. For bone tissue engineering, a porosity of about 90%, a pore size greater than 100 μm, and a high pore interconnectivity can be accepted as desirable for facilitating the attachment and proliferation of cells, the ingrowth of new tissue, and the vascularization of the new tissue formed.[26] Pineda et al.[27,28] reported that although polyester membranes with pore sizes up to 200 μm in diameter promoted bone growth within a 1-cm radii of defects in rabbits, smaller pore sizes promoted most growth. The pore size distribution results obtained from SEM images (Figure 1) confirmed that the pores were inhomogeneous and varied in the range of 5–200 μm. In Figure 2, the distribution curves of pore sizes for the scaffolds measured with the mercury porosimeter are given. From the plots, one can see that microporosities of PCL-50β/G were higher than those of the other samples. The fraction of bigger pores increased with increasing ratio of β-TCP/gelatin microspheres. For pure PCL scaffolds, the pore sizes were lower than those of the others. A broad pore distribution was obtained for the PCL-50β/G sample.

Compressive Properties of the Composite Scaffolds

The compressive modulus (E) and CS values for the 50% deformation of scaffolds in the dry and wet states are given in Table II.

As shown in the table, the modulus decreased significantly with increasing filler content. β-TCP is a hard inorganic material, and one can expect that the compressive properties would increase with the addition of β-TCP-containing microspheres. However, according to the SEM and pore size distribution results (Figures 1 and 2), the samples with higher filler amounts had larger porosities, and these pores reduced the mechanical properties of the matrix. In the wet state, the modulus values of all of the composite samples decreased more significantly with increasing filler content compared to the scaffolds in dry state. This phenomenon could be attributed to the swelling properties of gelatin and to the pore sizes. The penetration of aqueous media to the inner parts of the scaffolds led to the softening of the samples, and this decreased E. Moreover, aqueous media can also prevent the reinforcing properties of β-TCP because of its hydrophilicity. The CSs for the deformation of the 50% of scaffolds were 98, 76, 68, and 39 kPa for PCL-0, PCL-10β/G, PCL-30β/G, and PCL-50β/G, respectively. These values decreased for the wetted samples and were 94, 61, 52, and 27 kPa for PCL-0, PCL-10β/G, PCL-30β/G, and PCL-50β/G, respectively. All of the samples prepared in this study showed low compressive mechanical properties compared to cortical bone supports such as acrylic bone cements. Therefore, we suggest that they could be used in lower load-carrying bones of human body, such as the ones used in maxillofacial surgery.[29] In the literature, it has been reported that porous and biodegradable scaffolds with certain mechanical properties are widely used in hard tissue engineering.[30–32] The scaffolds prepared in this study as PCL composites with good bioactivity could be good candidates for this type of non-load-bearing bones and could be applied to bone defects of the head, neck, face, and so on.

Table II. Compressive Properties and E and CS Values at 50% Deformation

	Dry state (kPa)		Wet state (kPa)	
Sample	E	CS	E	CS
PCL-0	578 ± 125	98 ± 6	567 ± 110	94 ± 5
PCL-10β/G	293 ± 20	76 ± 4	199 ± 27	61 ± 9
PCL-30β/G	108 ± 35	68 ± 12	75 ± 17	52 ± 9
PCL-50β/G	55 ± 8	39 ± 8	38 ± 9	27 ± 7

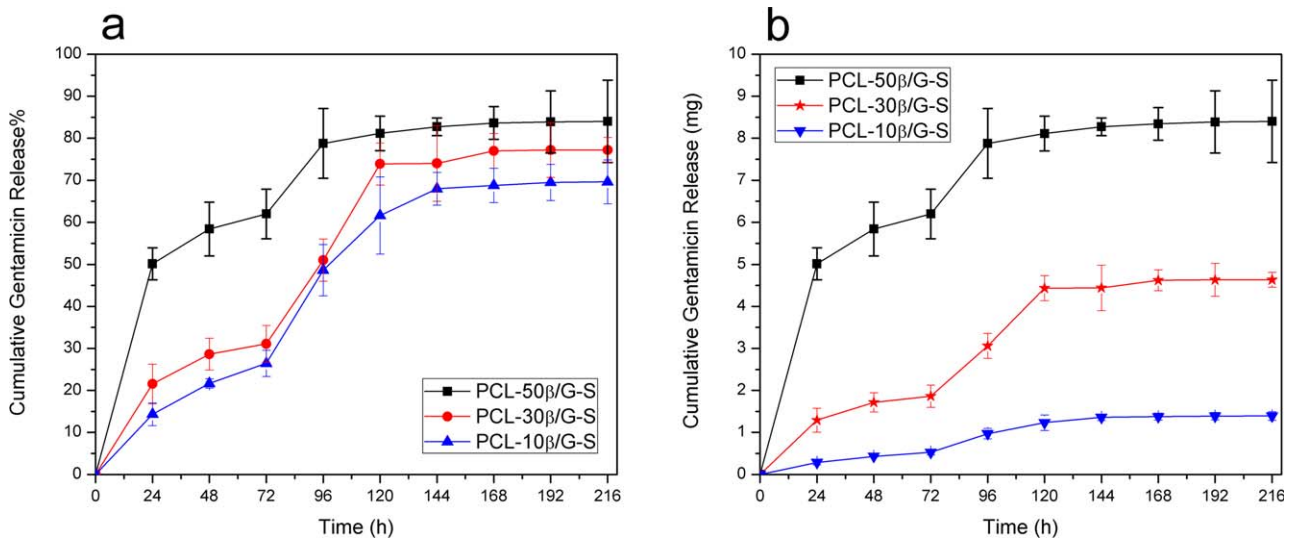

Figure 3. Cumulative gentamicin releases from composite scaffolds (S) in (a) percentage and (b) milligrams. [Color figure can be viewed in the online issue, which is available at wileyonlinelibrary.com.]

In Vitro Gentamicin Release from the Composite Scaffolds

The release behaviors of gentamicin from the composite scaffolds are shown in Figure 3. It has been reported that in local applications, antibiotic-release profiles should exhibit a high initial release rate to respond to the elevated risk of infection introduced during the initial shock and that the late release should be at a lower rate at an effective level.[33,34]

In this study, as shown in the release profiles, there were two steps. First, there was a burst effect for about 24 h followed by a slower step up to 72 h; then, there was a second fast release up to about 120 h. The burst release most probably was the result of the release of gentamicin entrapped on or in the gelatin coat of the microparticles. Gelatin can easily swell in aqueous media and let the drug diffuse out easily. The slow release result from gentamicin diffusing out from the inner parts of the microparticles. The second fast release took place because of the degradation of the matrix. The total drug-release amounts were found to be approximately 67, 74, and 87% of the total loaded drug content for PCL-10β/G, PCL-30β/G, and PCL-50β/G, respectively. The burst effect decreased as the filler content decreased. This effect was most probably caused by the effective entrapment of the microspheres into the PCL matrix in the case of lower filler contents. However, in the samples containing higher filler amounts, the microspheres created inhomogeneity and incomplete coating by the PCL matrix [as shown in Figure 1(h,l)], and therefore, a higher burst release of gentamicin was observed, as reported previously. The release rate and the amount of applied antibiotic can be adjusted by the modification of the composition of the scaffolds and the structure of microparticulate fillers.[24,25]

In Vitro Degradation Studies

The degradation studies of the scaffolds were carried out in buffer and lipase-containing media and showed the results of hydrolytic and enzymatic degradation, respectively. Gravimetric measurements gave information about the quantity lost, and SEM analysis showed morphological changes during degradation. The degradation of the matrices was studied for the PCL-0 and PCL-30β/G composites. The percentage weight loss of the hydrolytic and enzymatic degradation of these samples is given in Figure 4. As expected, no significant difference was observed in weight loss for the hydrolytically degraded samples of PCL-0 after 1 week, whereas about a 3% degradation was observed for PCL-30β/G. For the second case, this decrease most probably resulted from the dissolution of gelatin. However, for enzymatic degradation; 90.5% of PCL-0 and 50.3% of the PCL-30β/G composites degraded in 24 h. After 7 days, the weight loss of PCL-0 was greater than 90%, and the remaining amount was hardly detectable. For the same period, the percentage weight loss for the PCL-30β/G sample was 60.0%.

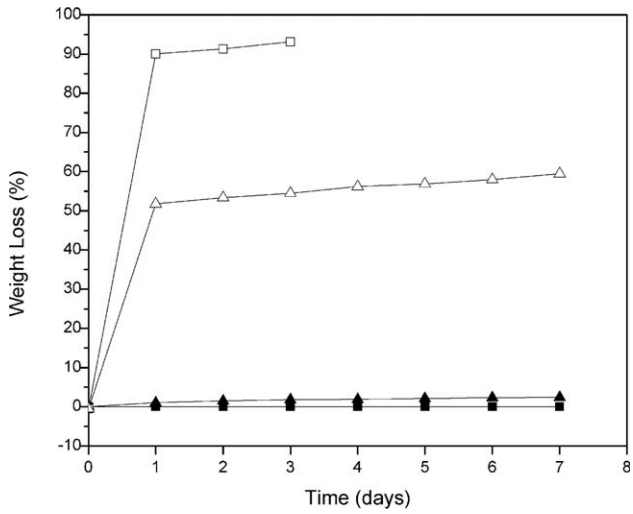

Figure 4. Hydrolytic degradation profiles in PBS [(▲) PCL-0 and (■) PCL-30β/G] and enzymatic degradation profiles in lipase-containing PBS [(□) PCL-0 and (△) PCL-30β/G].

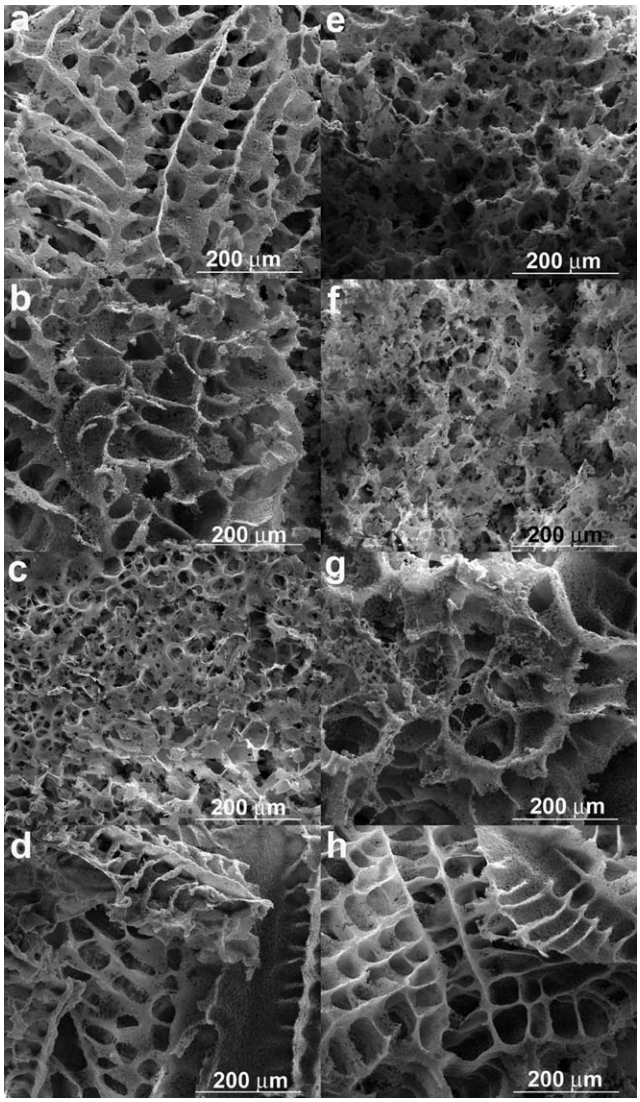

Figure 5. SEM images of the scaffolds after a degradation period of 1 week: (a–d) in PBS and (e–h) in lipase-containing PBS, (a,e) surface of PCL-0, (b,f) cross section of PCL-0, (c,g) surface of PCL-30β/G, and (d,h) cross section of PCL-30β/G.

The SEM images of the samples after hydrolytic and enzymatic degradation are given in Figure 5. In PBS media, the pure PCL scaffold did not show any significant degradation at the surface or in the cross-sectional area. For PCL-30β/G, although about a 3% decrease was observed by gravimetric analysis, we could not detect it in the SEM images. On the other hand, rapid enzymatic degradation was observed. For all of the scaffolds, destroyed and leached regions were observed at both the surface and cross-sectional area after 1 week of enzymatic degradation. Lipase degraded PCL with a fast kinetic.[6] The rapid degradation of PCL began with the surface, and the creation of pores on the surface led to the lipase enzyme penetrating the inner parts of the scaffolds. This led to significant weight loss. The morphological characteristics of the degraded PCL-30β/G samples showed partial degradation on the surface and in the bulk. The presence of inorganic TCP particles kept these matrices together and prevented their total degradation in the examined period.

Cell Attachment and Viability on the Composite Scaffolds

The numbers of Saos-2 cells on five different composite scaffolds were determined with MTT assay (Table I). Figure 6 presents the attachment [Figure 6(a)] and proliferation [Figure 6(b)] behavior of the Saos-2 cells.

To examine the attachment profile, an MTT test was performed after 1 day of incubation. To achieve attachment, the cells were incubated (2×10^4 cells per scaffold) without growth medium for 20 min after seeding; therefore, the cell numbers on day 1 were low for all of the samples, including the TCPS control [Figure 6(a)]. The number of cells attached on the surface of the TCPS control was lower than the number of cells attached on the scaffolds. The reason for the higher cell attachment on the scaffolds was most probably the larger surface area of the scaffolds, which was exposed to the cells more preferably. The cell numbers on PCL-50β/G (17×10^3) were the highest because of their more spongelike structure compared to those of the others.

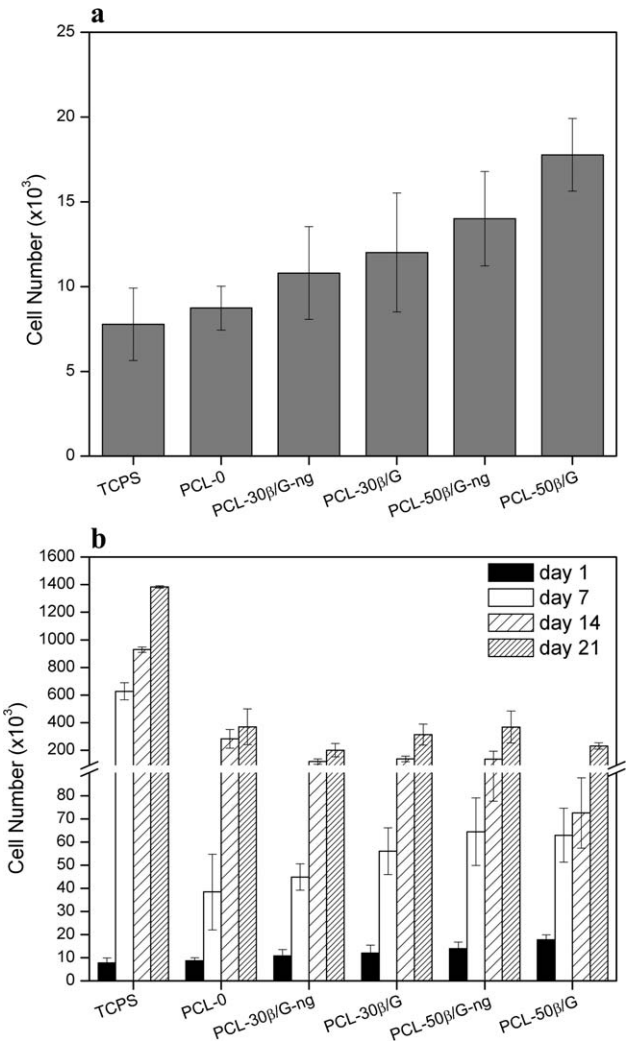

Figure 6. MTT assay for Saos-2 cells on the composite scaffolds: (a) attachment (day 1) and (b) proliferation trend of the cells [seeding density = 2×10^4 cells/cm^2 ($n = 3$)].

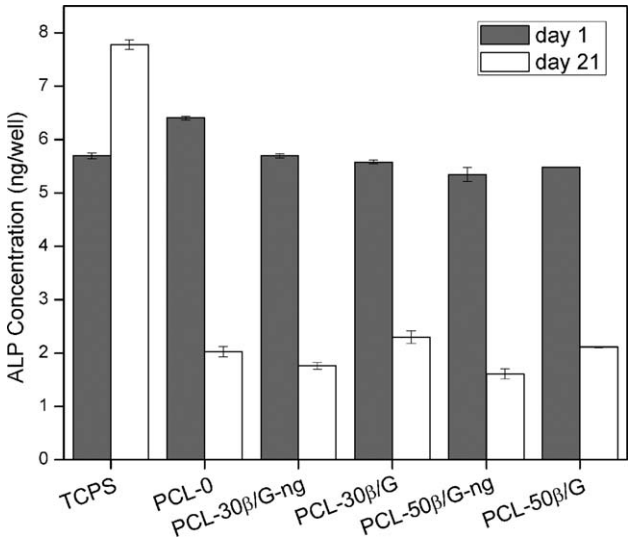

Figure 7. Alkaline phosphatase activities of the Saos-2 cells.

For the proliferation of Saos-2 cells, a very promising increase in cell number was observed for all of the scaffolds [Figure 6(b)]. The increase in the control TCPS was higher than that of the scaffolds. After a week, the number of cells demonstrated the same trend as the attached cell numbers on day 1. The highest number of cells was observed for the PCL-50β/G samples. This was caused by the presence of a higher amount of β-TCP/G microspheres, where the presence of gelatin enhanced cell proliferation.[35] Another reason may have been the leaching of some TCP particles on the first day, which created larger pores, which could be occupied by cells. At the end of day 21, the number of cells on all of the scaffolds were found to be around 200–300 $\times$ 10^3; this demonstrated good proliferation. The adhesion of cells to biomaterials is a major factor in their biocompatibility, and it has been postulated that the more compatible the surface is, the greater the cell attachment will be.[36,37] The composite scaffolds prepared in this study allowed the cells to attach and proliferate quite effectively.

Alkaline Phosphatase Activity of the Saos-2 Cells on the Composite Scaffolds

The osteoblastic phenotype expressions of Saos-2 osteosarcoma cells seeded on the scaffolds were studied by their expression of ALP activity (Figure 7). The ALP activities of the cells on all of the composite scaffolds were similar to the those of the control group on day 1, as expected. On the other hand, at the end of day 21, the ALP activity of only the control group increased, whereas the activities of the cells on the composite scaffolds decreased. This severe decrease might have been the result of the accumulation of cells in small pore volumes, which caused a stress effect on the cells. Similar results have also been reported in the literature.[38,39] The results show the presence of ALP activity, which is a critical phenotypic property of the bone cells and demonstrated the presence of bone cells in the scaffolds.

SEM

The cells on the composite scaffolds were examined by SEM on days 1 and 21, and the obtained SEM images are presented in Figures 8 and 9, respectively. The cells on day 1 were seen on the surface of all of the scaffolds because the porous structure of the scaffolds was suitable for cell attachment. Intercellular connections produced by the cells as cytoplasmic elongations were observed as fibers [Figure 8(a)]. On day 21, the PCL surface with the cell layer on top was observed [Figure 8(b,d,f,h,j)].

In addition, the degradation on the surface was observed because the enzymes produced by the cells were effective on PCL degradation. On the other hand, it was difficult to determine the cells (10–20 μm size) on the surfaces of the scaffolds in Figure 8. Therefore, images with larger magnification were obtained (Figure 9). The cells could be seen on the surfaces at the end of day 21. Anchoring processes were observed, which extended from the cells to the surface of the composite scaffolds [Figure 9(b)]. However, depending on the materials and morphological characteristics, the agglomerations of cells and

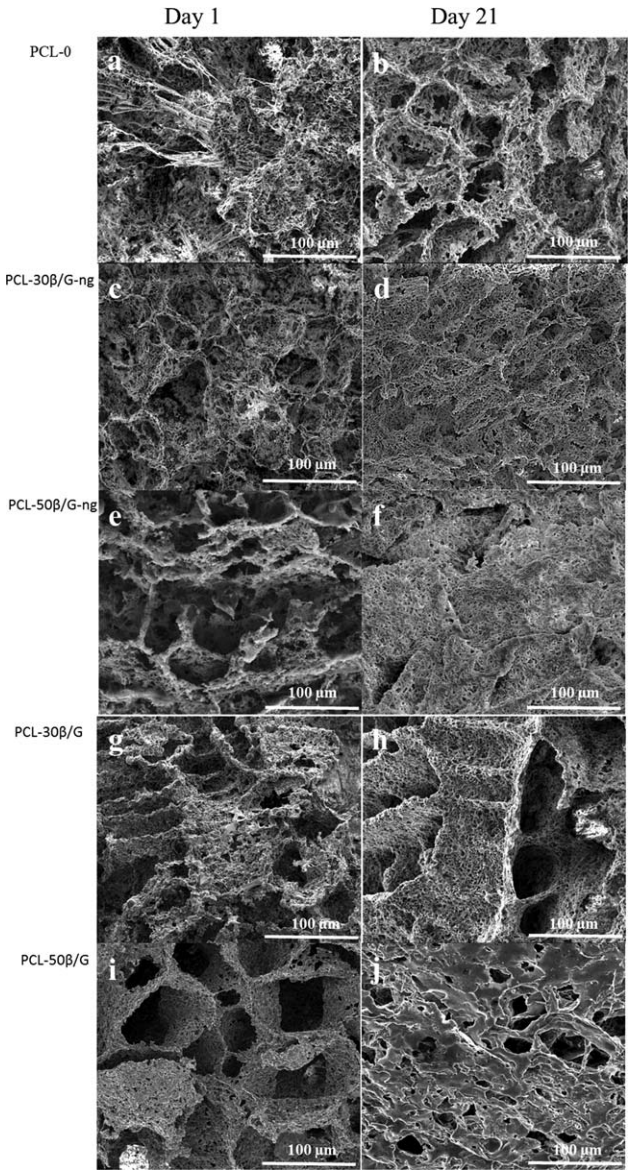

Figure 8. SEM micrographs of Saos-2 cells seeded on (a,b) PCL-0, (c,d) PCL-30β/G-ng, (e,f) PCL-50β/G-ng, (g,h) PCL-30β/G, and (i,j) PCL-50β/G scaffolds on days (a,c,e,g,i) 1 and (c,d,f,h,j) 21.

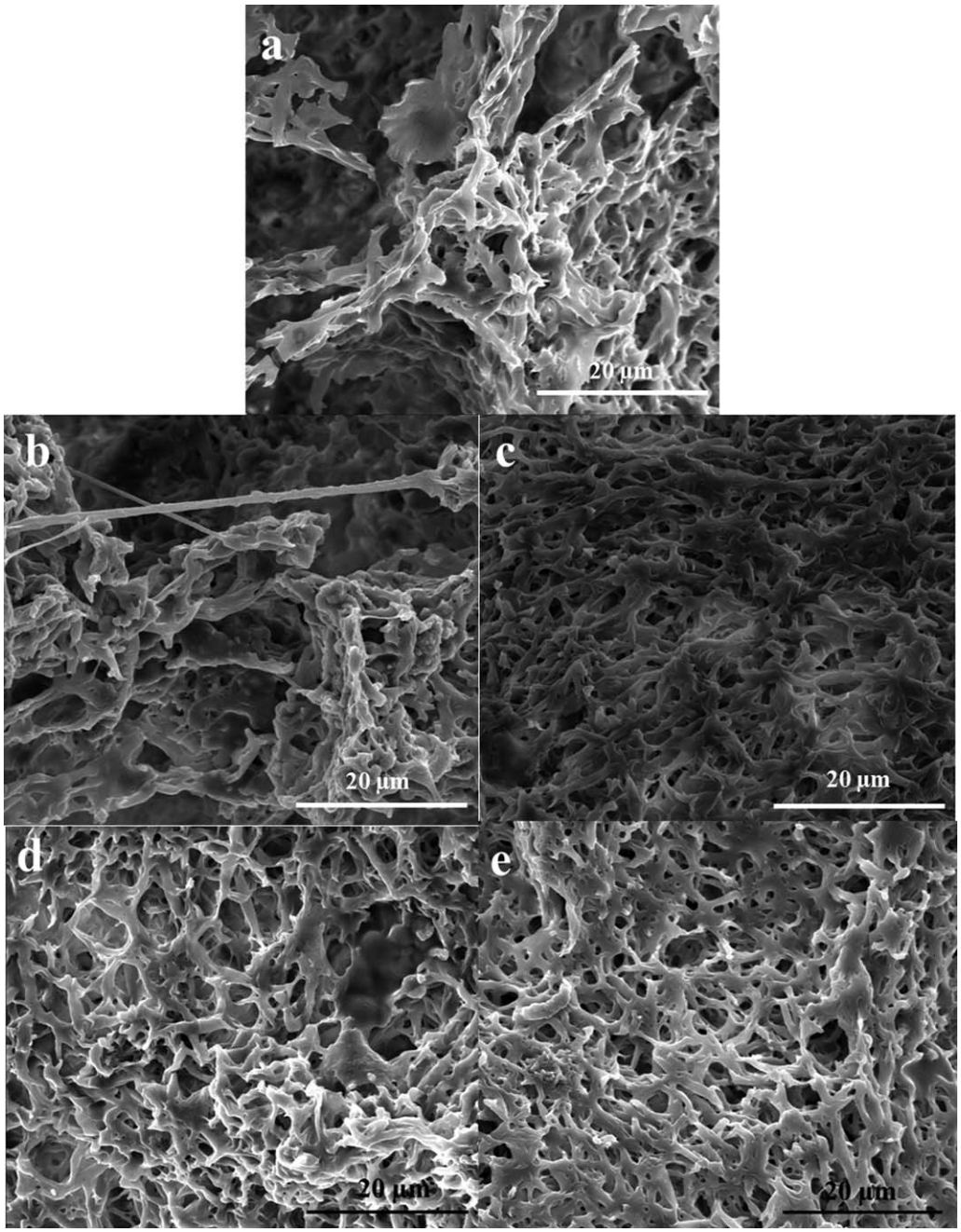

Figure 9. SEM micrographs of Saos-2 cells on day 21; (a) PCL-0, (b) PCL-30β/G-ng, (c) PCL-50β/G-ng, (d) PCL-30β/G, and (e) PCL-50β/G.

closing of pores could be observed. The cells on PCL-50β/G on day 21 covered the entire surface and closed the pores, as shown clearly in Figure 9(e).

Effect of the Saos-2 Cells on the Mechanical Properties of the Composite Scaffolds

The mechanical properties of the composite scaffolds after 21 days of Saos-2 cell culturing are given in Table III.

The CS values of PCL-30β/G during incubation in cell culture medium without and with cells and tested in the wet state were

Table III. Influence of the Saos-2 Presence on CS of the Composite Scaffolds (Values at 50% Deformation, Day 21)

Condition	PCL-30β/G CS (kPa)	PCL-50β/G CS (kPa)
Wet, no cells	56 ± 6	33 ± 5
Wet, with cells	62 ± 4	59 ± 9
Dry, no cells	68 ± 12	39 ± 8
Dry, with cells	154 ± 12	156 ± 9

found to be 56 ± 6 and 62 ± 4 kPa, respectively. Those values were similar to those found after incubation in PBS (52 ± 9 kPa), as given in Table II. For PCL-50β/G, during incubation in cell culture media without cells (33 ± 5 kPa) and with cells (59 ± 9 kPa), the values were significantly different than those of the original scaffold (27 ± 7 kPa). We concluded that the presence of cells enhanced the CS of the scaffold almost two times, even in the wet state.

However, for the scaffolds dried after the cell culture experiments, CS was found to be almost 2.5 folds higher than that of the wet states for both PCL-30β/G and PCL-50β/G. The main observation was that the presence of the cells increased the CSs of the scaffolds because of the deposition of extracellular matrix components.[40] In this study, because of the more porous structure of PCL-50β/G, which presented more area for the extracellular matrix proteins and cell incorporation, the deposition was more dominant compared to that of PCL-30β/G.

CONCLUSIONS

In this study, novel composite scaffolds were prepared by a freeze-drying technique for bone tissue engineering applications. Microparticulate fillers prepared from β-TCP and gelatin and loaded with gentamicin were added to PCL scaffolds to create multifunctionality. *In vitro* gentamicin release studies indicated an effective sustained release from the scaffolds. Both the dry- and wet-state compressive mechanical results were found to be sufficient for bone tissue engineering applications. Effective cell attachment and proliferation were observed for all of the scaffolds, and ALP activity at a certain level was also obtained. The scaffolds were good candidates for use in bone tissue engineering after the amounts of microparticulate fillers and gentamicin in the scaffold structure were optimized. In conclusion, it is possible to obtain multifunctional scaffolds with biodegradable, osteoconductive properties that are capable of delivering antibiotics.

ACKNOWLEDGMENTS

This study was supported by grant METU-BAP-07-02-2011-101.

REFERENCES

1. Ucar, S.; Yilgor, P.; Hasirci, V.; Hasirci, N. *J. Appl. Polym. Sci.* **2013**, *130*, 3759.
2. Guarino, V.; Ambrosio, L. *Acta Biomater.* **2008**, *4*, 1778.
3. Hou, Q. P.; Grijpma, D. W.; Feijen, J. *Biomaterials* **2003**, *24*, 1937.
4. Isikli, C.; Hasirci, V.; Hasirci, N. J. *Tissue Eng. Regen. Med.* **2012**, *6*, 135.
5. Heo, S.-J.; Kim, S.-E.; Wei, J.; Hyun, Y.-T.; Yun, H.-S.; Kim, D.-H.; Shin, J. W.; Shin, J.-W. *J. Biomed. Mater. Res. Part A* **2009**, *89*, 108.
6. Kızıltay, A.; Fernandez, A. M.; San Roman, J.; Hasirci, V.; Hasirci, N. *J. Biomater. Tissue Eng.* **2012**, *2*, 143.
7. Yilgor, P.; Sousa, R. A.; Reis, R. L.; Hasirci, N.; Hasirci, V. *J. Mater. Sci. Mater. Med.* **2010**, *21*, 2999.
8. Sun, H.; Mei, L.; Song, C.; Cui, X.; Wang, P. *Biomaterials* **2006**, *27*, 1735.
9. Kim, U. J.; Park, J.; Kim, H. J.; Wada, M.; Kaplan, D. L. *Biomaterials* **2005**, *26*, 2775.
10. Yilgor, P.; Sousa, R. A.; Reis, R. L.; Hasirci, N.; Hasirci, V. *Macromol. Symp.* **2008**, *269*, 92.
11. Schantz, J. T.; Hutmacher, D. W.; Ng, K. W.; Teoh, S. H.; Chim, H.; Lim, T. C. *Cell Transplant.* **2002**, *11*, 125.
12. Chuenjitkuntaworn, B.; Inrung, W.; Damrongsri, D.; Mekaapiruk, K.; Supaphol, P.; Pavasant, P. *J. Biomed. Mater. Res. Part A* **2010**, *94*, 241.
13. Dong, J.; Uemura, T.; Shirasaki, Y.; Tateishi, T. *Biomaterials* **2002**, *23*, 4493.
14. Sivakumar, M.; Panduranga, R. K. *Biomaterials* **2002**, *23*, 3175.
15. Ulubayram, K.; Kiziltay, A.; Yilmaz, E.; Hasirci, N. *Biotechnol. Appl. Biochem.* **2005**, *42*, 237.
16. Muvaffak, A.; Gürhan, I.; Hasirci, N. *J. Biomed. Mater. Res. Part B* **2004**, *71*, 295.
17. Krasko, M. Y.; Golenser, J.; Nyska, A.; Nyska, M.; Brin, Y. S.; Domb, A. J. *J. Controlled Release.* **2007**, *117*, 90.
18. Brin, Y. S.; Golenser, J.; Mizrahi, B.; Maoz, G.; Domb, A. J.; Peddada, S.; Tuvia, S.; Nyska, A.; Nyska, M. *J. Controlled Release* **2008**, *131*, 121.
19. Barrera-Méndez, F.; Escobedo-Bocardo, J. C.; Cortés-Hernández, D. A.; Almanza-Robles, J. M.; Múzquiz-Ramos, E. M. *Ceram. Int.* **2011**, *37*, 2445.
20. Zhang, Y.; Zhang, M. *J. Biomed. Mater. Res.* **2002**, *62*, 378.
21. Yilgor, P.; Hasirci, N.; Hasirci, V. *J. Biomed. Mater. Res. Part A* **2010**, *93*, 528.
22. Shi, M.; Kretlow, J. D.; Spicer, P. P.; Tabata, Y.; Demian, N.; Wong, M. E.; Kasper, F. K.; Mikos, A. G. *J. Controlled Release* **2011**, *152*, 196.
23. Francis, L.; Meng, D.; Knowles, J. C.; Roy, I.; Boccaccini, A. R. *Acta Biomater.* **2010**, *6*, 2773.
24. Aydemir Sezer, U.; Aksoy, E. A.; Durucan, C.; Hasirci, N. *Polym. Compos.* **2012**, *33*, 1644.
25. Aydemir Sezer, U.; Aksoy, E. A.; Hasirci, V.; Hasirci, N. *J. Appl. Polym. Sci.* **2013**, *127*, 2132.
26. Hutmacher, D. W. *Biomaterials.* **2000**, *21*, 2529.
27. Pineda, L. M.; Busing, M.; Meing, R. P.; Gogolewski, S. *J. Biomed. Mater. Res. Part A* **1996**, *31*, 385.
28. Tsuruga, E.; Takita, H.; Itoh, H.; Wakisaka, Y.; Kuboki, Y. *J. Biochem.* **1997**, *121*, 317.
29. Yilgor, P.; Yilmaz, G.; Onal, M. B.; Solmaz, I.; Gundogdu, S.; Keskil, S.; Sousa, R. A.; Reis, R. L.; Hasirci, N.; Hasirci, V. *J. Tissue. Eng. Regen. Med.* **2013**, *7*, 687.
30. Nam, Y. S.; Yoon, J. J.; Park, T. G. *J. Biomed. Mater. Res.* **2000**, *53*, 1.
31. Harris, L. D.; Kim, B. S.; Mooney, D. J. *J. Biomed. Mater. Res.* **1998**, *42*, 396.
32. Kim, S. E.; Cho, Y. W.; Kang, E. J.; Kwon, I. C.; Bae, L. E.; Kim, J. H.; Chung, H.; Jeong, S. Y. *Fibers Polym.* **2001**, *2*, 64.

33. Smith, K. L.; Schimpf, M. E.; Thompson, K. E. *Adv. Drug. Delivery Res.* **1990**, *4*, 343.

34. Zilberman, M.; Elsner, J. J. *J. Controlled Release* **2008**, *130*, 202.

35. Perez. A. A.; Valle, S. D.; Altankov, G.; Ginebra, M. P. *J. Biomed. Mater. Res. Part. B* **2011**, *97*, 156.

36. Hammett-Stabler, C. A.; Johns, T. *Clin. Chem.* **1998**, *44* 1129.

37. Anselme, K. *Biomaterials.* **2000**, *21*, 667.

38. Rodan, B. R.; Imai, Y.; Thiede, M. A.; Wesolowski, G.; Thompson, D.; Bar-Shavit, Z.; Shull, S.; Mann, K.; Rodan, G. A. *Cancer. Res.* **1987**, *47*, 4961.

39. Malaval, L.; Liu, F.; Roche, P.; Aubin, J. E. *J. Cell. Biochem.* **1999**, *74*, 616.

40. Freed, L. E.; Martin, I.; Vunjak-Novakovic, G. *Clin. Orthop.* **1999**, *367*, 46.